

Improvement of Precision in Strain Rate Measurement Using Spatial Distribution of Envelope of RF Echoes

Yu Obara^{1‡}, Shohei Mori², Masumi Iwai-Takano^{3,4,1}, Mototaka Arakawa^{1,2}, and Hiroshi Kanai^{2,1} (¹Grad. Sch. Biomed. Eng., Tohoku Univ.; ²Grad. Sch. Eng., Tohoku Univ.; ³Dept. Epidemiol., Fukushima Med. Univ.; ⁴Dept. Cardiovasc. Surg., Fukushima Med. Univ.)

1. Introduction

Ultrasound-based strain rate (SR) measurement has been studied for the non-invasive evaluation of myocardial function. The SR is calculated from the difference of the velocities along the depth direction in the myocardia. The velocities are not uniform in the depth direction when the thickness of each myocardium changes in the heart wall, *i.e.* the $SR \neq 0$. However, in conventional velocity estimators, it is assumed that the velocities are uniform within the velocity estimation window.

In the present study, by considering the change in thickness within the velocity estimation window, the influence on the velocity estimation was formulated to improve the precision of the SR measurement. The formulation was validated through the phantom experiment.

2. Principles

2.1 Influence of change in thickness on velocity estimation using ultrasound phase difference

Figure 1 shows the schematic of the velocity estimation. In the velocity estimator using the ultrasound phase difference, the phase difference is obtained from the angle of the summation of $z_i^* z_{i+1}$ using the analyzed signals at the i th and the $(i + 1)$ th frames, z_i and z_{i+1} [1]. Therefore, the estimated velocity at the interesting depth sample n is the average value of the true velocities $v_i(n)$ weighted with the envelopes of the RF signals within the window, that is, the true velocities at the depth sample with the high-amplitude envelope are dominant. As shown in Fig. 1, for example, the true velocities around the depth sample n_1 with the high-amplitude envelopes are dominant and the estimated velocity is biased toward $v_i(n_1)$.

2.2 Formulation of the bias error

In this section, a model is introduced to $\varphi_i(n, \Delta m, \varepsilon_i) =$

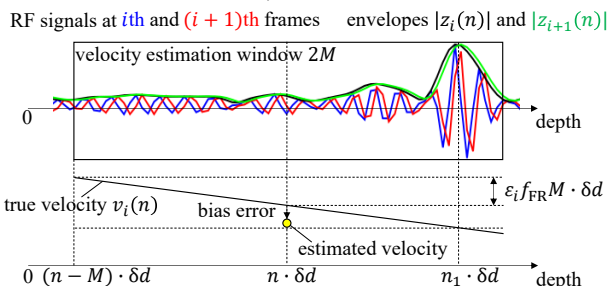


Fig. 1 Schematic of velocity estimation when thickness of each myocardium uniformly changes.

formulate the bias error contained in the estimated velocity, which is described in the Sect. 2.1. In the present study, the assumption is introduced that the thickness of each myocardium uniformly changes, *i.e.* the true velocity linearly changes along the depth direction, within the velocity estimation window. This assumption is weaker than that of the uniform velocities in conventional velocity estimators. Assuming that the influence of the interference of the multiple scattered waves is small, the analyzed signals obtained by the demodulation of the RF signal at the i th and the $(i + 1)$ th frames, $z_i(n)$ and $z_{i+1}(n)$, respectively, are formulated as follows.

$$z_i(n) = |z_i(n)|e^{j\theta_i(n)}, \quad (1)$$

$$z_{i+1}(n) = |z_{i+1}(n)|e^{j\{\theta_i(n)+\Delta\theta_i(n)\}}, \quad (2)$$

$$\theta_i(n) = 2\pi f_0 n T_s, \quad (3)$$

$$\Delta\theta_i(n) = -4\pi f_0 \frac{v_i(n)}{c_0 f_{FR}}, \quad (4)$$

$$v_i(n) = v_i(n - M) + \varepsilon_i f_{FR} M \cdot \delta d. \quad (5)$$

Here, n is the number of the depth sample points, $\theta_i(n)$ is the instantaneous phase, $\Delta\theta_i(n)$ is the phase difference between the consecutive frames, f_0 is the center frequency, T_s is the sampling period, c_0 is the speed of sound, f_{FR} is the frame rate, M is half the window length, ε_i is the strain, and δd is the inter-sample spacing.

The local velocity can be estimated using the phase of the cross-correlation function, $\angle r_i(\Delta m; n)$, which corresponds to the phase difference between $z_i(n)$ and $z_{i+1}(n + \Delta m)$.

$$\begin{aligned} \angle r_i(\Delta m; n) &= \angle \sum_{m=-M}^M z_i^*(n+m) \cdot z_{i+1}(n+m+\Delta m) \\ &= 2\pi f_0 \left\{ \Delta m T_s - \frac{2v_i(n)}{c_0 f_{FR}} \right\} + \varphi_i(n, \Delta m, \varepsilon_i), \end{aligned} \quad (6)$$

$$\angle r_i(\Delta m; n) = \angle \sum_{m=-M}^M |z_i(n+m)| |z_{i+1}(n+m+\Delta m)| e^{j2\pi f_0 \varepsilon_i m T_s}. \quad (7)$$

Here, Δm is the shift of the window between the frames and $\varphi_i(n, \Delta m, \varepsilon_i)$ is the phase difference caused by the change in thickness.

The velocity is estimated using the shift $\widehat{\Delta m}_n$ when the magnitude of the phase difference, $|\angle r_i(\Delta m; n)|$, is minimum. The estimated velocity $\widehat{v}_i(n)$ is determined as follows.

$$\begin{aligned}\hat{v}_i(n) &= \widehat{\Delta m}_n \cdot \delta d \cdot f_{FR} \\ &= v_i(n) + v_{e,i}(n, \widehat{\Delta m}_n, \hat{\varepsilon}_i) + \frac{c_0 f_{FR}}{4\pi f_0} \angle r_i(\widehat{\Delta m}_n; n),\end{aligned}\quad (8)$$

$$v_{e,i}(n, \widehat{\Delta m}_n, \hat{\varepsilon}_i) = -\frac{c_0 f_{FR}}{4\pi f_0} \varphi_i(n, \widehat{\Delta m}_n, \varepsilon_i), \quad (9)$$

$$\widehat{\Delta m}_n = \arg \min_{\Delta m} |\angle r_i(\Delta m; n)|. \quad (10)$$

In Eq. (8), the first term in the right hand is the true velocity $v_i(n)$, the second term is the bias error $v_{e,i}(n, \widehat{\Delta m}_n, \hat{\varepsilon}_i)$ caused by the change in thickness within the velocity estimation window, and the third term is the estimation error depending on the inter-sample spacing. If the inter-sample spacing is sufficiently small, the third term is close to zero. In this case, the bias error $v_{e,i}(n, \widehat{\Delta m}_n, \hat{\varepsilon}_i)$ caused by the change in thickness is the main cause of the error. Therefore, the bias error contained in the estimated velocity, $v_{e,i}(n, \widehat{\Delta m}_n, \hat{\varepsilon}_i)$, can be calculated using the spatial distributions of the envelopes ($|z_i(n)|$ and $|z_{i+1}(n)|$) and the strain ε_i as Eqs. (7) and (9).

3. Water Tank Experiment

Figure 2(a) shows the schematic of the water tank experiment. The sponge phantom was manually pressed by pushing the agar plate as shown in Fig. 2(a). The RF signals were obtained by the ultrasound diagnostic apparatus (F75, Aloka) with a sector probe of the 3-MHz center frequency f_0 and the 50-ns sampling period T_s . The frame rate f_{FR} was set at 250 Hz. Applying the fast Fourier transform to the RF signal, the interpolated analyzed signal was obtained. The velocity distribution was estimated with the 2.5-mm window ($2M \cdot \delta d$). The SR is estimated from the estimated velocities as follows.

$$\widehat{SR}_i(n) = \hat{\varepsilon}_i(n) \cdot f_{FR} = \frac{\hat{v}_i(n+M) - \hat{v}_i(n)}{M \cdot \delta d}. \quad (11)$$

If the pushing pressure and the elasticity of the sponge are constant, the true velocity linearly changes along the depth direction, *i.e.* the strain is constant. Thus, the assumed constant strain $\hat{\varepsilon}_i$ was manually determined from the M-mode image (Fig. 2(b)). The bias error $v_{e,i}(n, \widehat{\Delta m}_n, \hat{\varepsilon}_i)$ was estimated by Eqs. (7) and (9) using the spatial distributions of the measured envelopes ($|z_i(n)|$ and $|z_{i+1}(n)|$) and the assumed strain $\hat{\varepsilon}_i$ which is constant. The formulation of the bias error $v_{e,i}(n, \widehat{\Delta m}_n, \hat{\varepsilon}_i)$ was validated by comparing the estimated velocity $\hat{v}_i(n)$ to the velocity obtained by adding the estimated bias

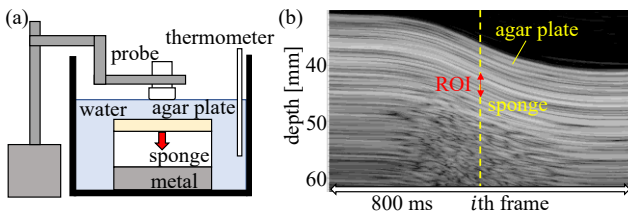


Fig. 2 (a) Schematic of water tank experiment, (b) the M-mode image at the center ultrasound beam.

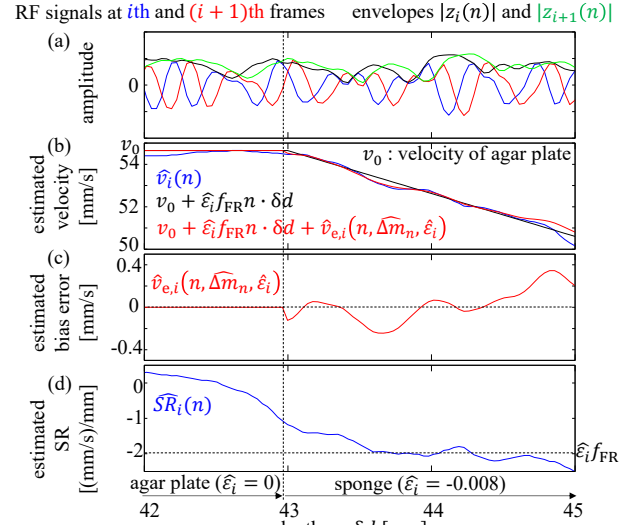


Fig. 3 (a) The RF signals and their envelope distributions, (b) the estimated velocities, (c) the estimated bias errors, and (d) the estimated SRs, in the region of interest (ROI) at the i th frame (red arrow in Fig. 2(b)). The estimated bias error was not zero in the sponge area (Fig. 3(c)). The assumed velocity corrected with the estimated bias error (red line in Fig. 3(b)) corresponded to the estimated velocity $\hat{v}_i(n)$ (blue line in Fig. 3(b)). Therefore, it was confirmed that the estimated velocities contained the bias errors formulated in Eqs. (7) and (9). The SR estimated from $\hat{v}_i(n)$ which contained the bias error was not constant in the sponge area (Fig. 3(d)). The bias errors would increase the variance of the estimated SRs. The consideration of the bias error improves the precision in both the velocity and SR estimations.

error $\hat{v}_{e,i}(n, \widehat{\Delta m}_n, \hat{\varepsilon}_i)$ to the assumed velocity corresponding to $\hat{\varepsilon}_i$.

4. Results and Discussion

Figure 3 shows (a) the RF signals and their envelope distributions, (b) the estimated velocities, (c) the estimated bias errors, and (d) the estimated SRs, in the region of interest (ROI) at the i th frame (red arrow in Fig. 2(b)). The estimated bias error was not zero in the sponge area (Fig. 3(c)). The assumed velocity corrected with the estimated bias error (red line in Fig. 3(b)) corresponded to the estimated velocity $\hat{v}_i(n)$ (blue line in Fig. 3(b)). Therefore, it was confirmed that the estimated velocities contained the bias errors formulated in Eqs. (7) and (9). The SR estimated from $\hat{v}_i(n)$ which contained the bias error was not constant in the sponge area (Fig. 3(d)). The bias errors would increase the variance of the estimated SRs. The consideration of the bias error improves the precision in both the velocity and SR estimations.

5. Conclusion

In this paper, the bias error of the estimated velocity caused by the change in thickness within the velocity estimation window was formulated. In our future works, we will propose the precise SR measurement method considering the bias error.

Acknowledgment – This work was partially supported by JSPS KAKENHI JP22J10644.

Reference

1. H. Hasegawa and H. Kanai: IEEE Trans. Ultrason. Ferroelectr. Freq. Control **55** (2008) 1921.